Improved Structure-Adaptive Anisotropic Filter Based on a Nonlinear Structure Tensor

Jie Wu[1,2], *Zuren Feng*[1], *Zhigang Ren*[3]

[1] *Laboratory for Manufacturing Systems Engineering, Xi'an Jiaotong University, Xi'an 710049, Shaanxi, China*
[2] *School of Electronic Information Engineering, Xi'an Technological University, Xi'an 710032, China*
[3] *Autocontrol Research Institute, Xi'an Jiaotong University, Xi'an, China*

Abstract: *A variety of structure-adaptive filters are proposed to overcome the blurred effects of image structures caused by the classical Gaussian weighted mean filter. However, two major issues are needed to be dealt with carefully for structure-adaptive anisotropic filters. One is to properly construct the filter kernel and the other is to accurately estimate the orientation of the image structures. In this paper we propose to improve the structure-adaptive anisotropic filtering approach based on the nonlinear structure tensor (NLST) analysis technique. According to the anisotropism measurements of image structures, a new kernel construction method is designed to make the filter shape fine adapted to image features. Through the accurately estimated orientation of the image structures, the filter kernels are then properly aligned to perform the filtering process. Experimental results show that the proposed filter denoises the noisy images carefully and image features, such as corners and junctions are well preserved. Compared with some other known filters, the proposed filter obtains great improvements both in Mean Square Error (MSE) and visual quality.*

Keywords: *Structure-adaptive anisotropic filter, non-linear structure tensor, image denoising, orientation estimation.*

1. Introduction

Computing denoised versions of noisy images have always been a desirable goal in the fields of computer vision and image processing. It is a useful pre-processing step that eases further analysis and processing of the considered image. Numerous filtering schemes have been proposed both in the image domain [1] and transformed domains [2]. Recently, anisotropic filtering schemes have especially drawn more attention by researchers in image processing communities, which enable us to reduce noise, at the same time, to keep important image structures neither delocalized nor blurred. Different approaches are proposed based on diffusion techniques [3, 5], structure-adaptive anisotropic filters [6, 7], and transform methods with anisotropic atoms [8, 11]. In this paper we focus on the anisotropic filtering methods in the image domain, which are inspired by a common idea: to penalize smoothing along the direction of maximum signal variation while it is favoured in the orthogonal one. By casting the problem in terms of a heat equation in anisotropic medium, P e r o n a and M a l i k [3] presented a nonlinear diffusion scheme. When small iteration steps are used, it can also be considered as a useful tool for image noise filtering [12]. However, the classical anisotropic diffusion model of Perona and Malik is actually referred to as a non-homogeneous isotropic diffusion model [13], which only considers the gradient information of the image and limits the smoothing of an image near pixels with a large gradient magnitude. To address this problem, real anisotropic diffusion was proposed to allow the diffusion to be different along different directions defined by the local geometry of the image [4, 14]. Thus, diffusion across edges can be prevented while diffusion along edges is being allowed. Diffusion methods suffer from three major drawbacks: i) they slow down the filtering process in very noisy images, ii) they tend to distort sloping edges [6], iii) the diffused results depend on the diffusion time which is hard to be determined [15]. Another kind of a structure-adaptive anisotropic filtering scheme has been proposed by Yang and co-workers [6]. Instead of using local gradients as means of controlling the anisotropism of filters, the anisotropic Gaussian filter is controlled by local intensity orientation and an anisotropic measure. But the parameter estimations in Yang's filtering scheme are non-optimal for images features, such as corners, junctions or edges.

In Yang's filtering scheme, there are two main operations during the anisotropic filtering process: constructing a proper Gaussian neighbourhood for signal estimation and estimating accurate orientation to align the anisotropic kernel along the local image structures. Either of them should be carefully done to obtain a high filtering quality. Yang and co-workers construct the filter kernel according to image local anisotropic features and their orientation estimation scheme is based on the fact that the power spectrum of an oriented pattern lies along a line through the origin in the Fourier domain, while the direction of the line is perpendicular to the dominant spatial orientation of the pattern. An improved version of Yang's filtering scheme has been proposed [7]. In the improved filtering scheme, the main axis of the filter kernel is constructed in an exponential manner and the structure orientation is estimated by using the method of D o n a h u e and R o k h l i n [16],

where a gradient-type operator is calculated in a small neighbourhood and then average taken over a larger window to obtain the oriented pattern direction.

Nowadays, the structure tensor is a very popular tool for image local structure analysis in computer vision and image processing [17, 18]. It can provide very useful information about the two main operations in the structure-adaptive anisotropic filtering methods [19]. However, the smoothing with a Gaussian kernel makes the classic Linear Structure Tensor (LST) suffer from the dislocation of edges and corners, leading to inaccurate estimation results near region boundaries. To address this problem, many techniques have been proposed to replace the Gaussian smoothing and generate some kinds of improved structure tensors [20, 24]. Among these, the NonLinear Structure Tensor (NLST) [24] based on an anisotropic nonlinear diffusion processes has shown its capability for presenting useful information of an image, such as homogeneous regions, edges, and corners. In this paper we propose to improve the structure-adaptive anisotropic filtering technique based on the NLST. Both with the local anisotropism measure and the more accurate structure orientation derived from NLST, a more robust-to-noise filter kernel is constructed and properly aligned along image local structures. The rest of the paper is organized as follows. In Section 2 the definition of the nonlinear structure tensor is presented and some of its properties are analyzed. The structure-adaptive anisotropic filter in [4] is briefly reviewed in Section 3. The improved structure-adaptive anisotropic filtering method is proposed in Section 4. Experimental results and discussions are then given in Section 5 for both synthetic and natural images at various degrees of additive white Gaussian noise. Finally, the paper is concluded in Section 6.

2. Nonlinear structure tensor

2.1. Nonlinear structure tensor estimation

Let f be the greyscale image. The LST, $\mathbf{S}_{\text{LST}}(\mathbf{x})$ at each pixel $\mathbf{x}$ is calculated by a convolution operator of a Gaussian kernel with the outer product of the image gradients:

$$(1) \quad \mathbf{S}_{\text{LST}}(\mathbf{x}) = G_\rho(\mathbf{x}) * \left(\nabla f(\mathbf{x}) \nabla f(\mathbf{x})^{\text{T}} \right) = \begin{pmatrix} G_\rho * f_x f_x & G_\rho * f_x f_y \\ G_\rho * f_x f_y & G_\rho * f_y f_y \end{pmatrix} = \begin{pmatrix} s_{11} & s_{12} \\ s_{12} & s_{22} \end{pmatrix}.$$

Symbol $*$ stands for the convolution operator, ∇ is the gradient operator, $G_\rho(\mathbf{x})$ is a Gaussian kernel with a standard deviation ρ.

The LST represented by the image gradients integrates information from the local neighbourhood without cancellation effects. The Gaussian smoothing of the initial matrix not only reduces the noise level in the matrix field, but also introduces spatial coherence through the scale factor ρ. The integration of local orientation creates additional information, thus making it possible to distinguish areas where the structures are oriented uniformly, as in regions with edges, from areas where the structures have different orientations, like in a corner region [24]. Unfortunately, linear Gaussian smoothing applied in the LST blurs and dislocates structures

114

because the local neighbourhood for the integration is fixed in both its size and its shape. Consequently, it cannot adapt to the data and the estimated orientation of a pixel located close to the boundary of two different regions is disturbed by ambiguous information. Recently, the NLST has been introduced [24], which is one of the adaptive structure tensors adapting the computation to the image data. The NLST uses the nonlinear diffusion process instead of Gaussian smoothing to overcome the above problem.

Since Gaussian smoothing can be modelled by the heat diffusion equation, Equation (1) is equivalent to the linear matrix-valued diffusion with the initial matrix

(2)
$$\mathbf{S}_0(\mathbf{x}) = \nabla f(\mathbf{x}) \nabla f(\mathbf{x})^{\mathrm{T}} = (s_{ij}^0),$$
$$\partial_t s_{ij} = \Delta s_{ij}, \ i, j = 1, 2.$$

The diffusion time t is related to the scale-space parameter ρ via $t = \rho^2 / 2$ and Δ stands for the Laplacian operator.

The NLST, $\mathbf{S}_{\mathrm{NLST}}(\mathbf{x})$, replaces the diffusion scheme (2) by the nonlinear diffusion process:

(3)
$$\partial_t s_{ij} = \mathbf{div}\left(g\left(\sum_{m,l=1}^{2} |\nabla s_{ml}|^2 \right) \nabla s_{ij} \right), \ i, j = 1, 2,$$

$g(\cdot)$ is a decreasing diffusivity function which correlates the amount of smoothing with the gradient of every component of the matrix data. Several diffusivity functions have been proposed in literature [4] and each of them is with different properties. In our case, we use the diffusivity function expressed as follows:

(4)
$$g(|\nabla f(\mathbf{x})|) = \frac{1}{\sqrt{|\nabla f(\mathbf{x})|^2 + \varepsilon^2}},$$

ε is a small positive constant to avoid singularities. The function is a good compromise between smoothing and edge preserving. Besides, there are also not so many parameters to be determined. We note that all matrix components of structure tensor are coupled in (3), which makes the NLST robust against noise or other artifacts, and allows a more reliable estimation in noisy images.

2.2. Interpretation of the nonlinear structure tensor

By smoothing the no-full rank initial matrices $\mathbf{S}_0(\mathbf{x})$ with the nonlinear diffusion process, the NLST becomes full rank. Thus, by using the eigenvalue decomposition, the structure tensor $\mathbf{S}_{\mathrm{NLST}}(\mathbf{x})$ can be expressed as follows:

(5)
$$\mathbf{S}_{\mathrm{NLST}}(\mathbf{x}) = (\mathbf{v}_1 \ \ \mathbf{v}_2) \begin{pmatrix} \lambda_1 & 0 \\ 0 & \lambda_2 \end{pmatrix} \begin{pmatrix} \mathbf{v}_1^{\mathrm{T}} \\ \mathbf{v}_2^{\mathrm{T}} \end{pmatrix},$$

$\mathbf{v}_1$, $\mathbf{v}_2$ are the eigenvectors of $\mathbf{S}_{\mathrm{NLST}}(\mathbf{x})$, and $\lambda_1 \geq \lambda_2 \geq 0$ are the eigenvalues of $\mathbf{S}_{\mathrm{NLST}}(\mathbf{x})$, corresponding to $\mathbf{v}_1$, $\mathbf{v}_2$.

The analysis of the eigenvalues and eigenvectors of $\mathbf{S}_{\mathrm{NLST}}(\mathbf{x})$ provides useful information about the complexity of local image structures in a neighbourhood [25]. The eigenvector $\mathbf{v}_1$ represents the direction of the maximum signal variation while $\mathbf{v}_2$ parallels to the direction of local oriented patterns. Furthermore, different cases in 2D can also be distinguished by analyzing the two eigenvalues:

i) $\lambda_1 \approx \lambda_2 \gg 0$: There is no preferred orientation of signal variation, which represents a corner, a junction in 2D or due to noise;

ii) $\lambda_1 \gg \lambda_2 \approx 0$: There is only one main direction of signal variation, where there may be a linear structure or an edge.

iii) $\lambda_1 \approx \lambda_2 \approx 0$: There is neither a preferred orientation of the signal variation nor significant variation, which corresponds to homogeneous regions. The total gradient energy is given by the trace of the structure tensor:

$$(6) \qquad \left| \nabla f(\mathbf{x}) \right|^2 = \mathrm{Trace}\left(\mathbf{S}_{\mathrm{NLST}}(\mathbf{x})\right) = \lambda_1(\mathbf{x}) + \lambda_2(\mathbf{x})$$

and an anisotropic measure is constructed as follows:

$$(7) \qquad C(\mathbf{x}) = \left(\frac{\lambda_1(\mathbf{x}) - \lambda_2(\mathbf{x})}{\lambda_1(\mathbf{x}) + \lambda_2(\mathbf{x})} \right)^2 .$$

The anisotropic measure indicates how much the local signal resembles a linear structure, and takes values between 0 and 1. Therefore, there may be a linear structure or an edge when $C(\mathbf{x}) \rightarrow 1$ and an isotropic or more complex case when $C(\mathbf{x}) \rightarrow 0$. The NLST is a very useful tool for adaptive and anisotropic processing systems and algorithms. We will present a new algorithm to denoise images using the information provided by the NLST to drive an anisotropic filtering kernel in Section 4.

3. The structure-adaptive anisotropic filter

The structure-adaptive anisotropic filter, which has been firstly proposed by Y a n g and co-workers [6], uses a local intensity orientation and an anisotropic measure of the level contours to control the shape and extent of the filter kernel. The filter kernel applied at each pixel $\mathbf{x}_0$ is defined as follows:

$$(8) \qquad k(\mathbf{x}_0, \mathbf{x}) = \phi(\mathbf{x} - \mathbf{x}_0) \times \exp\left\{ -\left[\frac{\left((\mathbf{x} - \mathbf{x}_0) \bullet \mathbf{n} \right)^2}{\sigma_1^2(\mathbf{x}_0)} + \frac{\left((\mathbf{x} - \mathbf{x}_0) \bullet \mathbf{n}_\perp \right)^2}{\sigma_2^2(\mathbf{x}_0)} \right] \right\}.$$

The symbol $\phi(\mathbf{x} - \mathbf{x}_0)$ represents a positive and rotationally symmetric cutoff function that satisfies the condition $\phi(\mathbf{x}) = 1$ when $|\mathbf{x}| \leq r$, and r is the maximum support radius. Both $\mathbf{n}$ and $\mathbf{n}_\perp$ are mutually normal unit vectors with $\mathbf{n}$ parallel to the local oriented pattern direction. The parameters of $\sigma_1(\mathbf{x}_0)$, $\sigma_2(\mathbf{x}_0)$ are used to control the shape of the kernel $k(\mathbf{x}_0, \mathbf{x})$. Furthermore, a relationship

$\sigma_1(\mathbf{x}_0) \geq \sigma_2(\mathbf{x}_0)$ is usually maintained to keep the kernel elongated along the direction $\mathbf{n}$.

The estimation of the oriented pattern direction $\theta(\mathbf{x})$ (the direction of vector $\mathbf{n}$) is done as follows:

(9)
$$\theta(\mathbf{x}) = \frac{1}{2}\tan^{-1}\left\{ \frac{\iint_\Omega 2\bullet\left(\frac{\partial f}{\partial x}\right)\left(\frac{\partial f}{\partial y}\right)dxdy}{\iint_\Omega \left(\left(\frac{\partial f}{\partial x}\right)^2 - \left(\frac{\partial f}{\partial y}\right)^2\right)dxdy} \right\} + \frac{\pi}{2},$$

where Ω is a local neighbourhood of the pixel $\mathbf{x} = (x, y)$.

The space parameters $\sigma_1(\mathbf{x})$ and $\sigma_2(\mathbf{x})$ are controlled by the corner detector $c(\mathbf{x})$ and the measurement of anisotropism $g(\mathbf{x})$ is as follows:

(10)
$$\sigma_1(\mathbf{x}) = \frac{r}{1 + c(\mathbf{x})/\beta},$$

(11)
$$\sigma_2(\mathbf{x}) = (1 - g(\mathbf{x}))\sigma_1(\mathbf{x}),$$

β is a normalization factor that controls how faithfully the corners and junctions are preserved during the filtering process.

The anisotropic measure gives indication of how strong a pattern is oriented. It is defined as follows:

(12)
$$g(\mathbf{x}) = \frac{\left\{\iint_\Omega \left(\left(\frac{\partial f}{\partial x}\right)^2 - \left(\frac{\partial f}{\partial y}\right)^2\right)dxdy\right\}^2 + \left\{\iint_\Omega 2\bullet\left(\frac{\partial f}{\partial x}\right)\left(\frac{\partial f}{\partial y}\right)dxdy\right\}^2}{\left\{\iint_\Omega \left(\left(\frac{\partial f}{\partial x}\right)^2 + \left(\frac{\partial f}{\partial y}\right)^2\right)dxdy\right\}^2}.$$

It can provide a feasible way of finding the corner and junction points within a given image. Yang and co-workers suggest using the measure of anisotropism and a gradient strength to estimate the corner strength in the following way:

(13)
$$c(\mathbf{x}) = (1 - g(\mathbf{x}))|\nabla f(\mathbf{x})|^2.$$

The parameter estimation approach of Yang's filter is essentially based on the LST. However, they used a fixed square window rather than a smoothly decaying Gaussian neighbourhood for information integration. This can enhance noise, introduce some artifacts, and make the parameter estimation inaccurate. In this paper, Yang's filtering scheme is utilized on the basis of LST for comparison.

4. Improved structure-adaptive anisotropic filter

In this section we propose improvement of the structure-adaptive anisotropic filter by using the information provided by the NLST. The filter kernel applied at each pixel $\mathbf{x}_0$ is defined as follows:

$$(14) \qquad G(\mathbf{x}_0, \mathbf{x}) = \exp\left\{-\frac{1}{2}\left[\frac{\left((\mathbf{x}-\mathbf{x}_0)\bullet\mathbf{n}\right)^2}{a^2(\mathbf{x}_0)} + \frac{\left((\mathbf{x}-\mathbf{x}_0)\bullet\mathbf{n}_\perp\right)^2}{b^2(\mathbf{x}_0)}\right]\right\}.$$

The symbols $\mathbf{n}$ and $\mathbf{n}_\perp$ have the same meaning as in (8). The parameters $a(\mathbf{x}_0)$ and $b(\mathbf{x}_0)$ represent the main axis and the orthogonal one of the anisotropic Gaussian kernel, respectively. A schematic drawing of the anisotropic Gaussian kernel is shown in Fig. 1 (a).
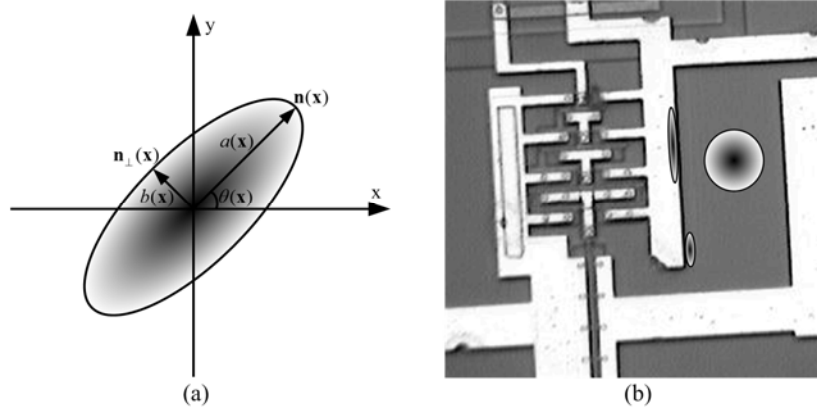
Fig. 1. An elliptic kernel controlled by its principle axes a, b and the direction θ (a); The filter kernel controlled through the image local anisotropic features (b)

The structure-adaptive anisotropic Gaussian filter is directional and adjusts the shape of the kernel according to the image local anisotropic features. The main purpose of such a filter is to make the flat areas well smoothed while keeping the edges less blurred and dislocated and the edge junctions scarcely destroyed. So the filter kernel must be carefully constructed and the orientation of image structures must be accurately estimated. The nonlinear structure tensor is just a very useful tool for this purpose. It provides a convenient way of finding edges, corners or junctions within a given image. The anisotropism measure $C(\mathbf{x})$ given in Section 2 can be a good indicator for edges. Furthermore, as learned from Yang's ideas, a measure of the corner strength can be calculated through the anisotropic measure $C(\mathbf{x})$ and the gradient strength $|\nabla f(\mathbf{x})|^2$:

$$(15) \qquad J(\mathbf{x}) = (1 - C(\mathbf{x}))|\nabla f(\mathbf{x})|^2 = \frac{4\lambda_1(\mathbf{x})\lambda_2(\mathbf{x})}{\lambda_1(\mathbf{x}) + \lambda_2(\mathbf{x})}.$$

The corner strength $J(\mathbf{x})$ is directly calculated with the eigenvalues of the structure tensor.

The anisotropic Gaussian kernel changes with its form, size and direction depending on the image local anisotropic features (Fig. 1 (b)). The main axis $a(\mathbf{x})$ must be maximal in regions with no corners and minimal in regions where there is a high value of the corner strength. Meanwhile, the second axis $b(\mathbf{x})$ must follow the

main axis $a(\mathbf{x})$ to become large in flat regions and shrink its value when regions with edges or junctions are met. Therefore, small filter kernels are used in regions with corners ($J(\mathbf{x}) \gg 0$), while large ones – for $J(\mathbf{x}) \to 0$. Large filter kernels are distinguished yet in two very different cases. The filter shape obtains a highly oriented elliptical form with its main axis parallel to the direction of local oriented patterns in regions with a high anisotropism measure ($C(\mathbf{x}) \to 1$) while extending its size isotropically to the maximal one for very flat regions. Furthermore, the preservation of the corner structures should also be carefully dealt with while maximizing the filtering capability. So, the transition of $a(\mathbf{x})$ from smooth regions to regions with corners should be taken good care of. To meet these requirements, the proposed adaptive filtering scheme is finally formalized as follows:

$$(16) \qquad a(\mathbf{x}) = r \cdot \left\{ 1 - \exp\left(-\frac{C_m}{\left(J(\mathbf{x})/\beta \right)^m} \right) \right\},$$

$$(17) \qquad b(\mathbf{x}) = \left(1 - C(\mathbf{x}) \right) a(\mathbf{x}),$$

where the parameters r and β take the same meanings as in Yang's filtering scheme and β is usually chosen as a value between 50% and 200% of the maximum corner strength within the image.

The determination function of the main axis $a(\mathbf{x})$ is first introduced by Weickert as the conductance function for his anisotropic diffusion model [4]. Therein, it is presented as follows:

$$(18) \qquad \varphi(s) = 1 - \exp\left(\frac{-C_m}{\left(s/\lambda \right)^m} \right).$$

The constant C_m is calculated in such a way that the flux-function $s\varphi(s)$ is increasing for $s \in [0, \lambda]$ and decreasing for $s \in (\lambda, \infty)$. To the proposed filtering scheme, the smoothing performance is prior for $J(\mathbf{x})/\beta \in (0, 1]$, while inhibited for the preservation of corners for $J(\mathbf{x})/\beta \in (1, \infty)$. These requirements are just similar to what the conductance function requires. Thus, by setting $s = J(\mathbf{x})/\beta$ and $\lambda = 1$, the constant C_m can be simply determined through the following equation:

$$(19) \qquad 1 - \exp\left(-C_m \right)\left(1 + mC_m \right) = 0.$$

Comparing the behaviour of the proposed space parameter $a(\mathbf{x})$ (equation (16)) with Yang's space parameter $\sigma_1(\mathbf{x})$ (equation (10)) highlights the improvement of the proposed filtering scheme.
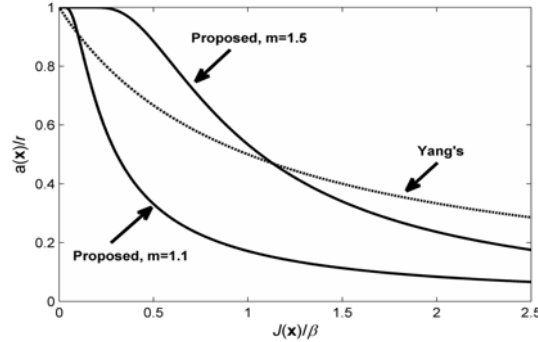
Fig. 2. Behaviours of controlling the main axis of the filter kernel
for Yang's filter and the proposed filter

Fig. 2 demonstrates the behaviour of controlling the main axis of the filter kernel for both Yang's filter and the proposed one. This figure shows that adopting the proposed filter can give better behaviours according to the corner strength. Compared with Yang's filter, the main axis $a(\mathbf{x})$ of the proposed anisotropic filter kernel takes larger values for low values of corner strength, and vice versa. Therefore, much more pixels are collected for estimation in smooth regions and only a few are used in regions with corners. So the proposed filter can produce smoother results in flat places and better preserve corners and junctions in images. In addition, the proposed kernel construction technique is with an extra parameter m, which allows the filtering characteristic adjusted for different noise levels and different image contents. Commonly, the parameter m takes its value between $(1, 1.5]$ and takes larger values for very noisy conditions and small ones for slightly corrupted images.

Accurate estimation of oriented pattern direction is of great importance for efficient performance of directional filters, such as the structure-adaptive anisotropic filter. If the orientation of the kernel is not properly aligned for anisotropic filtering, the image produced could be worse than that of using a simple linear filtering technique. Fortunately, the structure tensor allows orientation estimation and especially the NLST, which is robust against noise, can give a more reliable estimation with few blurring or dislocation effects. We propose to use the NLST for the estimation of oriented pattern direction. The orientation $\theta(\mathbf{x})$ is given by the eigenvector $\mathbf{v}_2$, which corresponds to the minimum eigenvalue λ_2 of the structure tensor $\mathbf{S}_{\text{NLST}}(\mathbf{x})$:

$$(20) \qquad \theta(\mathbf{x}) = \tan^{-1}\left\{ 2s_{12} / \left(s_{11} - s_{22} - \sqrt{(s_{11} - s_{22})^2 + 4s_{12}^2} \right) \right\}.$$

5. Experimental results and discussions

The performance of the proposed structure-adaptive anisotropic filter based on the NLST is compared with the same filtering scheme based on the LST, Yang's filter and the anisotropic diffusion filter. Experiments were conducted with several grey

120

scale test images shown in Fig. 3, including a synthetic image and three natural images – Cameraman, Bike and Circuit board, all of which are with the size 256×256.
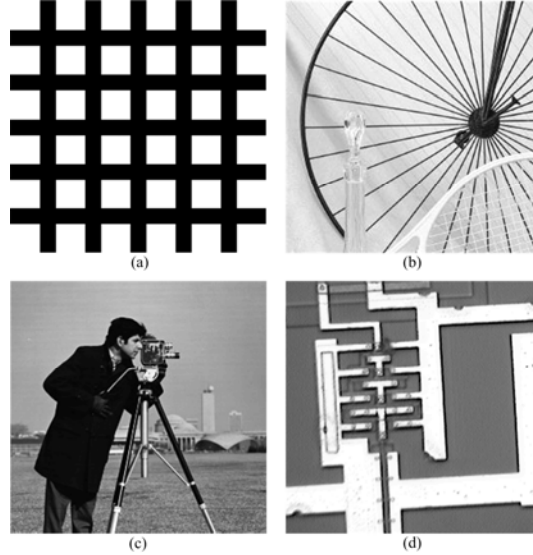

Fig. 3. Test images: Synthetic (a); Bike (b); Cameraman (c); Circuit Board (d)

Zero mean Gaussian white noises with standard deviation σ =15, 25, 35 were added to generate noisy images at different noise levels. The same parameters r and β are chosen for the proposed filter and Yang's filter, where the maximum axis size r was chosen as 2.0 and the parameter β was set to be 75% of the maximum of corner measures within the image [6]. Besides, the exclusive parameter m for the proposed filter kernel construction scheme was set to be 1.15, which will be proven to produce visually good results for these test images. The scale factor ρ for the LST was selected as 3.0. And we adopted the Edge Enhancing Diffusion (EED) filter [4] as the anisotropic diffusion filter. The diffusivity function along the oriented pattern direction was chosen as

$$(21) \qquad d(\mathbf{x}, t) = 1 / \left(1 + \frac{|\nabla f|^2}{K^2} \right).$$

And the one in the orthogonal direction was $d(\mathbf{x}, t)/5$. The conductance parameter K was set to be 10% of the maximum of the gradient magnitudes within the image [26]. The diffusion time t was carefully chosen to obtain visually good results.

Since the maximum size of the anisotropic filter kernel is determined by the corner strength measure, it is necessary to accurately locate and calculate the corner strength to achieve good filtering results. According to formula (15), the estimation of the corner strength based on the LST and NLST is compared. Both the LST and NLST were applied to the synthetic image and the results are presented in Fig. 4.
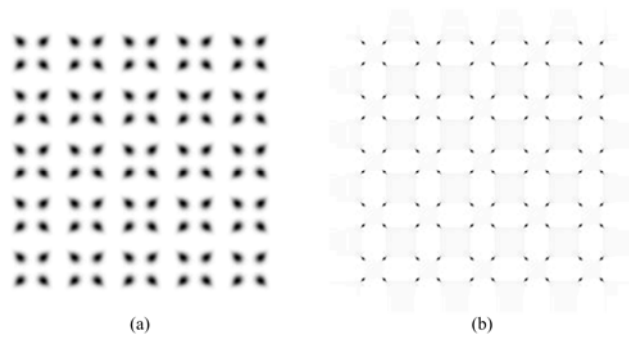
(a)   (b)

Fig. 4. Results of the corner strength estimation for synthetic image using techniques:
LST (a); NLST (b)

It can be seen that the corner location obtained with the LST is spread and less precise while the one obtained with the NLST is well localized. Moreover, efficient performance of the directional filters depends highly also on the correct estimating of the direction of oriented patterns. The performance of estimating the orientation based on the LST and NLST is compared as well. A noisy version of the bike image (σ =25), in which the orientation of lines is clearly distinguished, is used for the experiment.
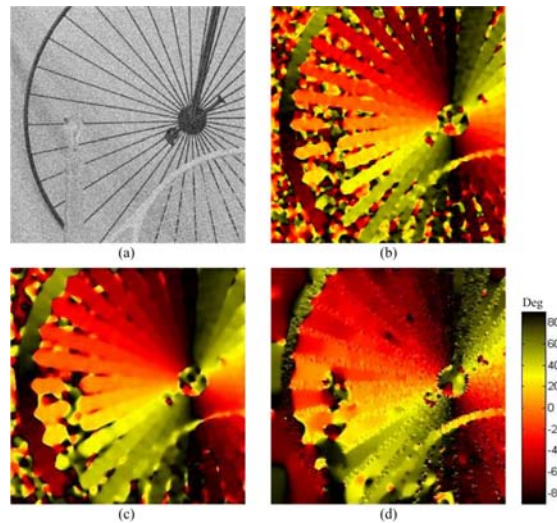

Fig. 5. Results of oriented pattern direction estimation using different techniques:
Bike image corrupted by Gaussian noise ($\sigma = 25$) and local orientation estimated by (a);
LST with $\rho = 2.0$ (b); LST with $\rho = 3.0$ (c); NLST (d)

As demonstrated in Fig. 5, the LST leaves too much noise in the orientation space when using a small scale factor ρ, and introduces blurs and dislocations to image structures when a larger one is used. Compared with the results of the LST, the estimated orientation with the NLST is more robust to noise, and shows more accurate directions for oriented patterns and more spatially consistent orientations for non-textural regions. Through these experiments it can be seen that both the location of corners and the estimation of structure orientations with NLST are superior to those with the LST.

122

Table 1. MSE values of denoised images using different methods

Image	σ	Noisy image	EED filter	Yang's filter	Proposed (LST)	Proposed (NLST)
Synthetic	15	226.213	35.764	98.461	47.848	21.345
	25	624.911	70.629	153.531	103.238	54.424
	35	1228.1	112.034	233.368	173.901	102.958
Bike	15	224.169	262.734	154.344	107.207	83.995
	25	622.821	444.687	218.889	196.295	149.024
	35	1232.5	648.496	320.572	316.051	249.723
Cameraman	15	224.295	82.806	100.969	68.808	59.396
	25	623.745	144.216	127.978	108.394	101.667
	35	1227.0	196.911	177.931	162.651	152.151

Table 1 shows the MSE values of the denoised images using different methods versus a range of noise levels. The proposed structure-adaptive anisotropic filter outperforms the other methods. Firstly, when the proposed filtering scheme based on the LST and Yang's filter are compared, remarkable MSE value improvement is obtained with the proposed filtering scheme, which demonstrates the improvement of our kernel construction approach. Secondly, the proposed filtering scheme based on the NLST produces better results than the one based on the LST, which indicates superior performance of NLST in the description of image structures. Both of these show that great improvements are achieved with the proposed filter when compared with Yang's filter.
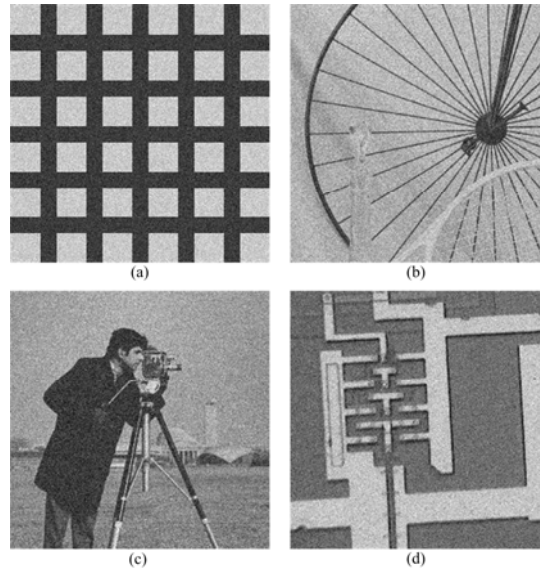

Fig. 6. The noisy images (a)-(d) obtained by adding white Gaussian noise ($\sigma = 25$) to test images in Fig. 3 respectively

To visually compare the denoising performance, the noisy versions of the test images at noise level $\sigma = 25$ (Fig. 6) are used and the denoised results by different methods are shown in Figs 7, 8, 9 and 10, respectively.
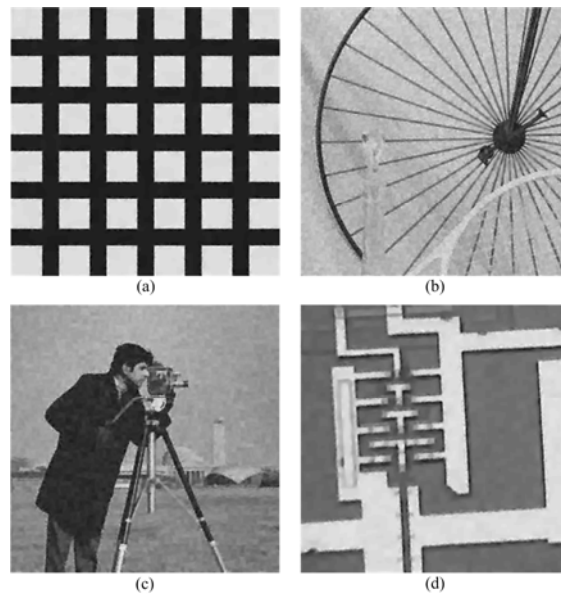
Fig. 7. The reconstructed images (a)-(d) by applying the EED filter
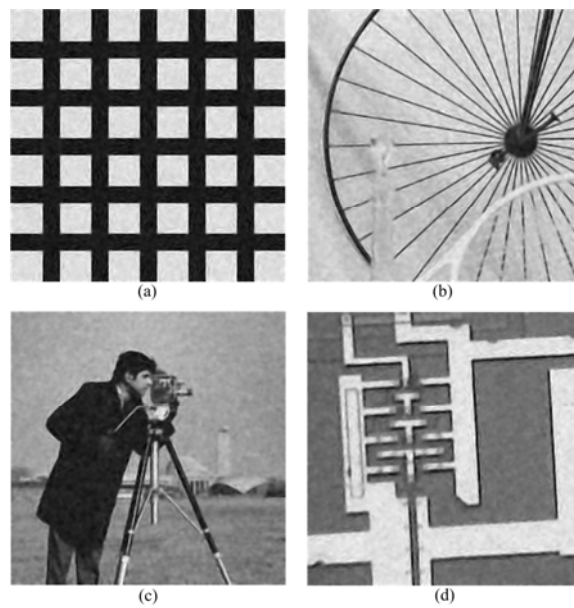to the noisy images in Fig. 6 respectively

Fig. 8. The reconstructed images (a)-(d) by applying Yang's filter
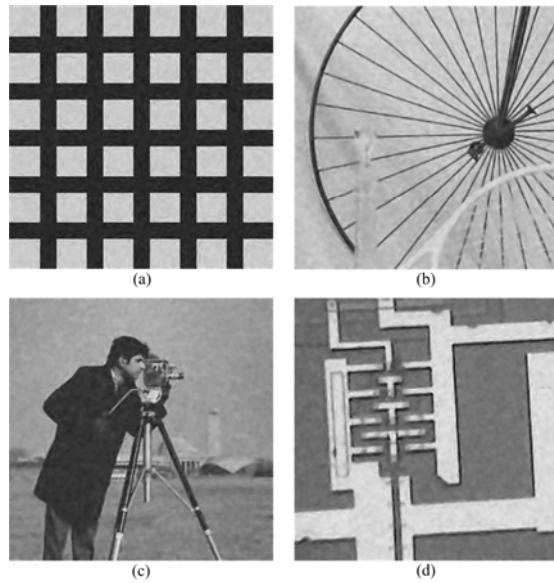to the noisy images in Fig. 6 respectively

Fig. 9. The reconstructed images (a)-(d) by applying the proposed filtering scheme based on the LST to the noisy images in Fig. 6 respectively
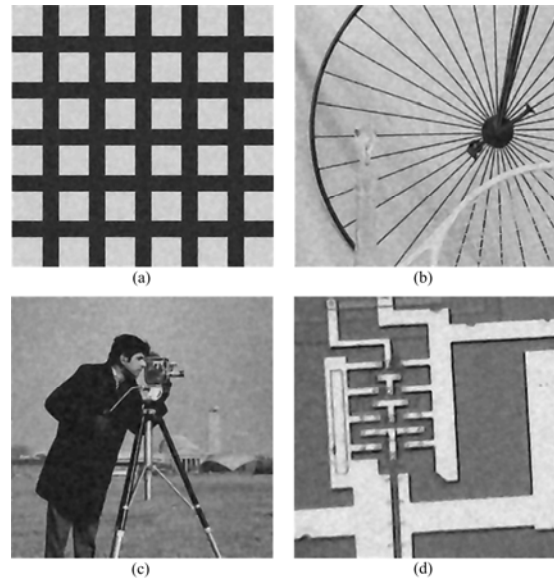

Fig. 10. The reconstructed images (a)-(d) by applying the proposed filtering scheme based on the NLST to the noisy images in Fig. 6 respectively

As seen, the anisotropic diffusion filter leaves much noise at edges and introduces some unexpected artifacts and block effects. Both Yang's filter and the proposed filter are able to overcome these problems. However, Yang's filter tends to produce artifacts along singularity structures like edges and lines. The proposed filter produces visually the best results and outperforms Yang's filter especially at corner regions and flat places.

6. Conclusions

An improved structure-adaptive anisotropic filtering scheme has been proposed, and this scheme is based on the NLST analysis of image structures. In the proposed filtering scheme, the NLST has been used to measure the image local anisotropic features and estimate the orientation of the image structures. The image anisotropism measurements are taken to shape the anisotropic Gaussian kernels and the filter kernels are then tuned to align along the structure orientations. The proposed filter could adapt its shape exquisitely to local image structures and denoise noisy images and image structures, such as corners, junctions and edges, are better preserved. The experiment on test images shows the excellent capability of the proposed filter for recognizing the image features and estimating structure orientations. The proposed filter carefully denoises the corner and edge regions and causes little blurs to these features. When compared to Yang's filter, the proposed filter not only obtains significant MSE value improvements, but also gets better visual quality. Furthermore, both the anisotropic diffusion filter and the proposed filtering scheme on the basis of LST are also taken for comparison. The former leaves much noise along the edges, while the latter introduces blurs to image features, such as corners and edges. The experimental results highlight the superior performance of the proposed structure-adaptive anisotropic filter based on the NLST.

R e f e r e n c e s

1. L i m, J. S. Two-Dimensional Signal and Image Processing. Englewood Cliffs, NJ, Prentice Hall, 1990.
2. E l a d, M., M. A. T. F i g u e i r e d o, Y. M a. On the Role of Sparse and Redundant Representations in Image Processing. – In: Proceedings of the IEEE, Vol. **98**, 2010, 972-982.
3. P e r o n a, P., J. M a l i k. Scale-Space and Edge Detection Using Anisotropic Diffusion. – IEEE Trans. on Pattern Analysis and Machine Intelligence, Vol. **12**, 1990, 629-639.
4. W e i c k e r t, J. Anisotropic Diffusion in Image Processing.– Stuttgart, Teubner-Verlag, 1998.
5. T s c h u m p e r l e, D., R. D e r i c h e. Vector-Valued Image Regularization with PDEs: A Common Framework for Different Applications. – IEEE Trans. on Pattern Analysis and Machine Intelligence, Vol. **27**, 2005, 506-517.
6. Y a n g, G. Z., P. B u r g e r, D. N. F i r m i n, S. R. U n d e r w o o d. Structure Adaptive Anisotropic Image Filtering. – Image and Vision Computing, Vol. **14**, 1996, 135-145.
7. G r e e n b e r g, S., D. K o g a n. Improved Structure-Adaptive Anisotropic Filter. – Pattern Recognition Letters, Vol. **27**, 2006, 59-65.
8. S t a r c k, J. L., E. J. C a n d e s, D. L. D o n o h o. The Curvelet Transform for Image Denoising. – IEEE Trans. on Image Processing, Vol. **11**, 2002, 670-684.
9. D o, M. N., M. V e t t e r l i. The Contourlet Transform: An Efficient Directional Multiresolution Image Representation. – IEEE Trans. on Image Processing, Vol. **14**, 2005, 2091-2106.
10. E a s l e y, G., D. L a b a t e, W. Q. L i m. Sparse Directional Image Representations Using the Discrete Shearlet Transform. – Applied and Computational Harmonic Analysis, Vol. **25**, 2008, 25-46.

11. L i m, W. Q. The Discrete Shearlet Transform: A New Directional Transform and Compactly Supported Shearlet Frames. – IEEE Trans. on Image Processing, Vol. **19**, 2010, 1166-1180.
12. G e r i g, G., O. K ü b l e r, R. K i k i n i s, F. A. J o l e s z. Nonlinear Anisotropic Filtering on MRI Data. – IEEE Trans. on Medical Imaging, Vol. **11**, 1992, 221-232.
13. W e e r a t u n g a, S. K., C. K a m a t h. A Comparision of PDE-Based Nonlinear Anisotropic Diffusion Techniques for Image Denoising. – In: Proc. SPIE Electronic Imaging, Image Processing: Algorithms and Systems II, Vol. **5014**, 2003, 201-212.
14. W e i c k e r t, J. A Review of Nonlinear Diffusion Filtering. – Lecture Notes in Computer Science, Vol. **972**, Berlin, Springer, 1997, 3-28.
15. M r á z e k, P., M. N a v a r a. Selection of Optimal Stopping Time for Nonlinear Diffusion Filtering. – International Journal of Computer Vision, Vol. **52**, 2003, 189-203.
16. D o n a h u e, M. J., I. R o k h l i n. On the Use of Level Curves in Image Analysis. – Image Understanding, Vol. **57**, 1993, 185-203.
17. B i g u n, J., G. H. G r a n l u n d, J. W i k l u n d. Multidimensional Orientation Estimation With Applications to Texture Analysis and Optical Flow. – IEEE Trans. on Pattern Analysis and Machine Intelligence, Vol. **13**, 1991, 775-790.
18. B r o x, T., R. v a n d e n B o o m g a a r d, F. L a u z e, J. v a n d e W e i j e r, J. W e i c k e r t, P. M r á z e k, P. K o r n p r o b s t. Adaptive Structure Tensors and Their Applications. – Visualization and Processing of Tensor Fields. Berlin, Germany, Springer-Verlag, 2005, 17-47.
19. C a s t a n o-M o r a g a, C. A., J. R u i z-A l z o l a. Anisotropic Filtering with Nonlinear Structure Tensors. – In: Proc. SPIE Real-Time Image Processing, Vol. **6064**, 2006, 215-223.
20. D o r e, V., R. F. M o g h a d d a m, M. C h e r i e t. Non-Local Adaptive Structure Tensors. Application to Anisotropic Diffusion and Shock Filtering. – Image and Vision Computing, Vol. **29**, 2011, 730-743.
21. Z h a n g, L., L. Z h a n g, D. Z h a n g. A Multi-Scale Bilateral Structure Tensor Based Corner Detector. – Lecture Notes in Computer Science, Vol. **5995**, 2010, 618-627.
22. H a n, S., W. T a o, D. W a n g, X. C. T a i, X. W u. Image Segmentation Based on GrabCut Framework Integrating Multi-Scale Nonlinear Structure Tensor. – IEEE Trans. on Image Processing, Vol. **18**, 2009, 2289-2302.
23. H a h n, J., C. O. L e e. A Nonlinear Structure Tensor with the Diffusivity Matrix Composed of the Image Gradient. – Journal of Mathematical Imaging and Vision, Vol. **34**, 2009, 137-151.
24. B r o x, T., J. W e i c k e r t, B. B u r g e t h, P. M r á z e k. Nonlinear Structure Tensors. – Image and Vision Computing, Vol. **24**, 2006, 41-55.
25. F e r n á n d e z, J. J., S. L i. An Improved Algorithm for Anisotropic Nonlinear Diffusion for Denoising Cryo-Tomograms. – Journal of Structural Biology, Vol. **144**, 2003, 152-161.
26. V a n d e n B o o m g a a r d, R. Algorithms for Nonlinear Diffusion Matlab in a Literate Programming Style. 2001.
    http://staff.science.uva.nl/~rein/nldiffusionweb/material.html.